A voyage through the deformed Earth with the self-consistent model

Modelling Simul. Mater. Sci. Eng. **7** (1999) 699–722. Printed in the UK PII: S0965-0393(99)01912-9

A voyage through the deformed Earth with the self-consistent model

Hans-Rudolf Wenk

Department of Geology and Geophysics, University of California, Berkeley CA 94720, USA

E-mail: wenk@seismo.berkeley.edu

Received 6 December 1998, accepted for publication 13 January 1999

Abstract. The viscoplastic self-consistent (VPSC) large strain polycrystal plasticity theory proved to be very useful for modelling the deformation in Earth materials. In contrast to most metals, rocks are composed of low-symmetry minerals with few slip systems. Also, most minerals have a high strain-rate sensitivity. Consequently, different orientations deform at different rates, contrary to the assumptions of the traditional Taylor model. The self-consistent method has been applied to predict textures and microstructures in many mineral systems and some highlights will be reviewed.

Starting at the surface of the Earth, *ice* deforms mainly by basal slip. Texture patterns observed in experiments and in the large polar ice sheets are well predicted with the VPSC model. In sediments, concentrations of salt (*halite*) deform by buoyant upwelling into salt domes. When VPSC was applied to halite, entirely different textures were predicted than those with the Taylor model, in better accordance with low temperature deformation experiments where $\{110\}\langle 1\bar{1}0\rangle$ is the prevalent slip system. *Calcite* has been an excellent example to illustrate how textures measured in natural rocks can be used to infer the deformation history in the Earth's crust. In calcite, VPSC automatically simulates the effects of 'curling' in axial compression, producing plane strain deformation at the microscopic scale. Many minerals are recrystallized. VPSC has been used as the basis of a model for dynamic recrystallization which balances nucleation of highly deformed grains and growth of less deformed grains. Applying it to *quartz* made it possible to explain textures in naturally deformed quartzites, particularly those deformed in simple shear. The upper mantle of the Earth is largely composed of *olivine* and deforms in large convection cells that extend over thousands of kilometres. Polycrystal plasticity predicts a highly heterogeneous texture evolution along streamlines with strong development of preferred orientation. Since single crystals of olivine are elastically anisotropic, oriented polycrystals also display anisotropy. Predicted anisotropies of seismic wave velocities of 5–10% in the model mantle agree well with those observed by seismologists. Finally the still highly enigmatic inner core is composed of solid ε*-iron* (hexagonal close packed) and seismologists have observed that wave velocities are slightly higher parallel to the Earth's axis than in the equatorial plane. Again, VPSC simulations suggest that this anisotropy in the centre of the Earth could be due to deformation during convection.

The examples illustrate, on a grand scale, that VPSC has not only helped us to unravel the deformation history of the Earth but also contributes towards to a better understanding of the deformation behaviour of complex and anisotropic materials.

1. Introduction

For some time polycrystal plasticity theory been used to model the deformation behaviour of geological materials. The applications of the Taylor–Bishop–Hill theory to halite (Siemes 1974) and quartz (Lister *et al* 1978, Lister and Hobbs 1980) laid the groundwork for more refined models. However, it soon became apparent that the low crystal symmetry and the

0965-0393/99/050699+24$30.00

limited numbers of slip systems restricted the application of this model that requires each crystal to deform at the same rate, irrespective of orientation. In addition, many minerals have a high strain-rate sensitivity. It was a lucky coincidence that Gilles Canova was visiting Los Alamos during ICOTOM 9 when the author was on research leave. He suggested a use for the viscoplastic self-consistent theory (VSPC) which had been developed by him and his co-workers at the University of Metz (Molinari *et al* 1987). This was at a time when problems with deformation simulations of minerals emerged: simulated pole figures of quartz showed little resemblance to those observed in natural rocks and in calcite it was not possible to simulate textures produced in a simple compression experiment. Clearly these materials did not satisfy the assumptions of the basic Taylor–Bishop–Hill theory (Taylor 1938), i.e. to deform homogeneously in a rigid-plastic fashion. For the following ten years Canova lent his expertise to Earth scientists to help them investigate mineral deformation. The author was fortunate to become closely associated with him and applied the self-consistent model to a number of Earth materials, not only improving simulations of mineral systems but also learning, from these applications, many characteristics of crystal deformation. In this paper we wish to summarize some of Canova's work and his contributions that have led geologists to a better understanding of deformation, affecting literally every rock type from ice on the surface of the Earth to hexagonal iron in the inner core, from single phase rocks such as limestone to polyphase composites such as granite.

In this paper we start on the surface and progress to increasingly deeper parts, highlighting some of the fascinating material aspects of the different systems. Compared to most metals, the Earth is a very complex system, structurally and compositionally heterogeneous at all scales. However, a common feature of most parts is that they deform according to principles of polycrystal plasticity. Except for the liquid outer core, most of the Earth is in the solid state. Figure 1 gives a cross section illustrating the major units; surface (hydrosphere), crust, mantle and core. Only rocks from the surface, crust and upper mantle can be sampled and are available for direct observation. For the rest evidence is indirect. Such indirect geophysical data suggest that deformation occurs also in the deeper parts of the Earth and that anisotropy is produced during convection. To the uninitiated, rocks appear brittle and crystal plasticity does not seem to apply. However, at high pressures and temperatures most rocks become ductile and the low diffusion constant is compensated for by slow strain rates (10^{-12} s^{-1}). With this in mind, most rocks are rather similar in their behaviour to metals as has been summarized in deformation mechanism maps (Frost and Ashby 1982).

This paper will not cover all aspects of rock deformation but centre on accounts for applications of the VPSC theory to rocks. Also, as far as the verification of the model and comparison with experimental and natural data goes, we will concentrate on texture (crystallographic preferred orientation) which is a sensitive and robust criterion. For a more detailed discussion the reader is referred to the monograph by Kocks *et al* (1998).

2. Ice: a crystal with few slip systems—surface of the earth

Ice H_2O covers a large portion of the Earth's surface. It occurs in the large polar ice caps, in glaciers, as seasonal snow and oceanic sheets. In most cases natural ice is deformed and exhibits texture that has been studied extensively (Kamb 1959, Herron and Langway 1982, Lipenkov *et al* 1989, Tison *et al* 1994). The strong textures suggest that models for the flow of ice must include the mechanical anisotropy due to crystal orientation.

Ice-I with a hexagonal crystal structure is peculiar in that it deforms almost exclusively on a single slip system (basal slip $(0001)\langle 11\bar{2}0\rangle$) and plasticity models such as Taylor, that require

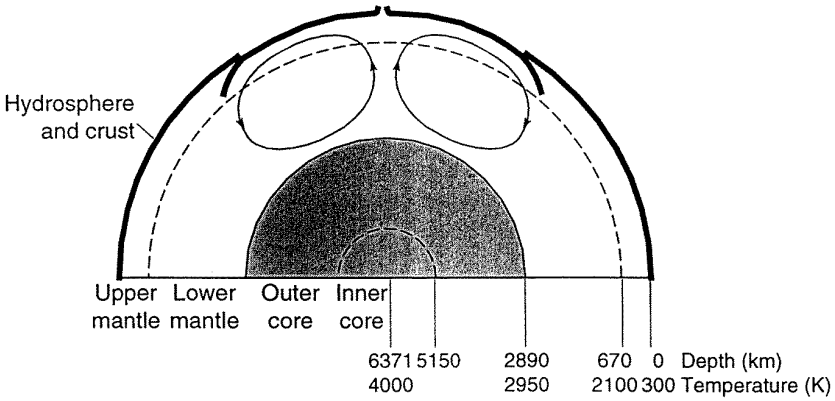

Figure 1. Schematic cross section, illustrating the structure of the Earth. Only the outer core is in a largely liquid state. Large convection cells, driven by temperature gradients, exist in the mantle and possibly in the inner core. They produce subduction of the lithosphere at trenches and uprising of lava near ridges. Two convection cells are shown.

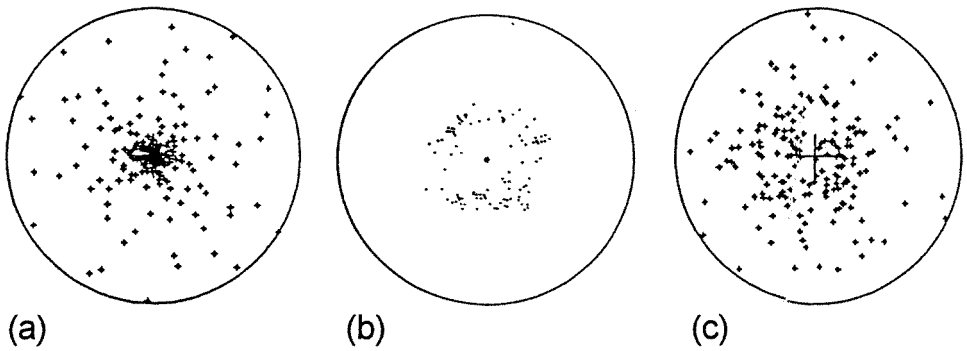

Figure 2. 0001 pole figures for ice, deformed in compression. The compression axis is in the centre of the pole figure. (a) VPSC deformation simulation to 39% strain, (b) experimentally deformed ice in compression (Castelnau *et al* 1996a), (c) natural deformation texture of ice from the GRIP drill core in the Greenland ice sheet (990 m) (Castelnau *et al* 1996b).

homogeneous deformation to maintain compatibility, are not applicable. After modelling attempts with kinematic concepts were unsatisfactory (e.g. Azuma and Higashi 1985, Alley 1988, Lipenkov *et al* 1989), the VPSC model provided the first convincing predictions for the development of preferred orientation in ice due to dislocation glide. For axial compression the deformation model predicts a high [0001] concentration near the compression axis (Castelnau *et al* 1996b, 1997) (see figure 2(a), centre of pole figure) and this agrees with observations from experiments (Duval 1981) (figure 2(b)) and cores from the Greenland ice sheet (Castelnau *et al* 1995) (figure 2(c)). During simple shear a [0001] maximum that is slightly oblique to the shear direction is predicted, again consistent with experimental data (Bouchez and Duval 1982).

However, there are several problems with modelling the deformation of ice: in many situations ice deforms near the melting point and diffusion is significant. This is expressed in pervasive recovery and recrystallization (Duval and Castelnau 1995). As will be shown in a later section, the self-consistent model can also be used to model recrystallization (Wenk *et al*

1997).

Ice does not only exist on the surface of the Earth but is an important constituent of the solar system. It is thought that it composes some of the moons of Jupiter, such as Ganimede, and of Saturn, such as Triton. At these conditions it does not exist in the same form as on Earth but in low-temperature and high-pressure modifications. Deformation of ice at low temperature and high pressure has been studied with experiments at 200 MPa and textures of rhombohedral ice-II were measured by neutron diffraction. Slip systems were determined by comparing measured textures with results from VPSC modelling (Bennett *et al* 1997).

3. Halite ('salt'): heterogeneous deformation—evaporite deposits

Cubic halite NaCl (also 'rock salt' or 'table salt') occurs in the Earth as evaporite sediments. If the saline water in all oceans evaporated, the sea floor would be covered with a 60 m thick layer of NaCl. However, during subsidence of an evaporite basin large deposits can form, extending over several kilometres in thickness. When these deposits are buried under rocks, salt, due to its low gravity, intrudes as salt domes into overlying strata and becomes deformed. Excellent examples are in southern Iran where salt domes are exposed on the surface. Since salt mines have gained recognition as potential repository sites for nuclear waste, the long-term deformation behaviour of halite has become of particular importance and numerous studies have been devoted to investigating the ductility of mono- and polycrystalline halite.

Halite deforms at low temperature preferentially by slip on $\{110\}\langle 1\bar{1}0\rangle$; other systems such as $\{100\}\langle 011\rangle$ and $\{111\}\langle 1\bar{1}0\rangle$ have at low temperature a five times higher critical resolved shear stress and are rarely activated (Carter and Heard 1970). In spite of the high cubic crystal symmetry, the preferred $\{110\}\langle 1\bar{1}0\rangle$ system has only two independent variants and therefore does not satisfy the von Mises criterion. In order to obtain an arbitrary shape change, harder systems need to be activated. One would expect that crystals which are favourably oriented for weak $\{110\}\langle 1\bar{1}0\rangle$ slip, i.e. those near (001) in an extension experiment, deform more than others, contrary to assumptions of the Taylor model that all grains maintain the same shape.

It was, therefore, natural to choose halite as a test case for the VPSC theory that allows differently oriented crystals to deform at different rates (Wenk *et al* 1989b). In contrast, to most other systems investigated so far, results for low-temperature deformation of halite for the Taylor and the self-consistent model are entirely different. The Taylor theory predicts extension axes to rotate towards (111) (figure 3, upper row) whereas the self-consistent theory predicts rotations towards (001) (figure 3, lower row). The difference in texture can be understood in terms of slip system activities. The Taylor maximum at (111) is caused by significant $\{111\}\langle 1\bar{1}0\rangle$ slip, required to maintain compatibility. In fact this hard system accommodates, on average, most of the strain. In the self-consistent case practically only $\{110\}\langle 1\bar{1}0\rangle$ is active, even though other systems were also allowed, resulting in a (001) texture. The self-consistent texture is close to that observed in extrusion experiments (Skrotzki and Welch 1983) (figure 4).

Predicted texture development is slower with the self-consistent model than with the Taylor model. The reason for this is that in the particular case of $\{110\}\langle 1\bar{1}0\rangle$ slip, for each system $\{110\}\langle 1\bar{1}0\rangle$ there is a complementary system $\{1\bar{1}0\}\langle 110\rangle$ (slip plane normal and slip direction exchanged) with the same absolute value of the Schmid factor. The shears on these systems compensate each other's spins. Superficially it may appear that no rotations should occur and no texture should develop. However, individual grain shapes are another cause for grain rotations and in the VPSC model these shapes vary, depending on orientation. Indeed, at low strain with similar grain shapes, the self-consistent texture is weak, but as the orientation-dependent grain shape distribution evolves, texture develops. With increasing strain some grains become strongly elongated and, for those, rotation increments are large as can be seen

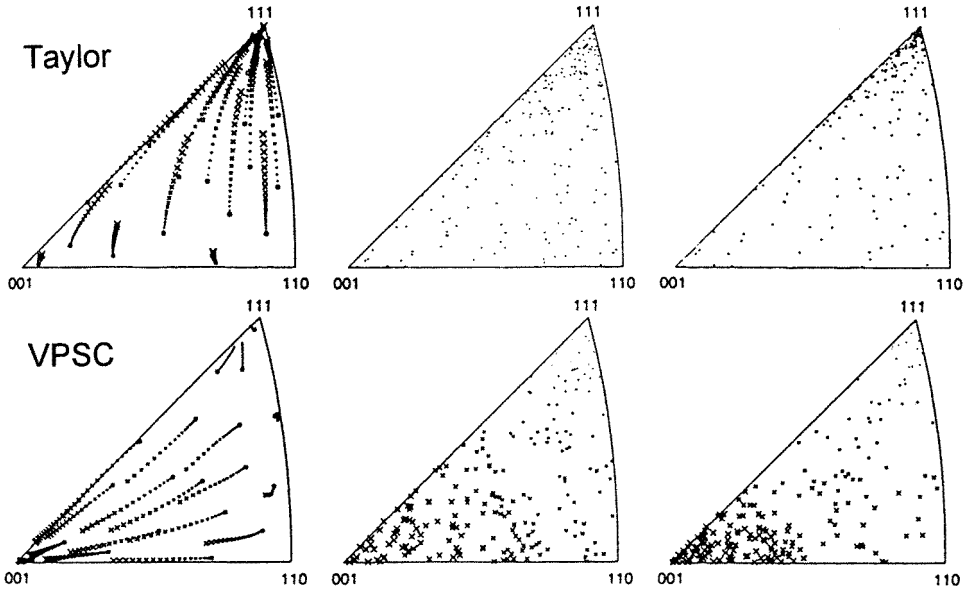

Figure 3. Texture development of halite in axial extension, according to the Taylor model (top) and the viscoplastic self-consistent theory (VPSC, bottom) with no work hardening. The first column shows the rotation trajectories for 20 representative orientations (in 5% strain increments), the second column gives distribution of 200 grains after 50% strain and the third column after 100% strain. The size of the symbols indicates the relative grain integrated plastic deformation (Wenk *et al* 1989b).

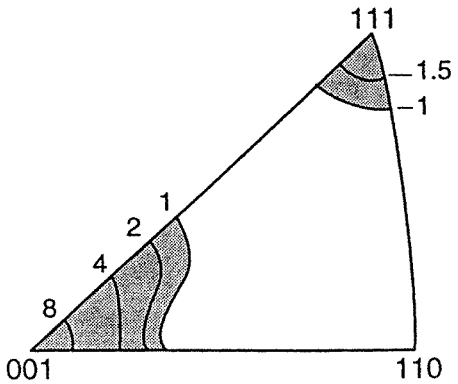

Figure 4. Inverse pole figure for experimentally extruded halite at 23 °C (Skrotzki and Welch 1983). Region above 1 m.r.d. (multiples of a random distribution) is shaded, contours are labelled. Stereographic projection.

in the rotation trajectories.

In figure 3 the symbol size is indicative of the deformation of individual grains as defined by an 'average grain shape parameter' ε_{av}. In Taylor simulations all grains deform by the same amount and at a given deformation step the grain shape of all grains is identical. In self-consistent calculations, grains near (001) deform much more (large symbols) than those near (111). At 100% extension, ε_{av} for Taylor simulations is 1.2, for self-consistent simulations it ranges from 0.3 to 2.3.

A more detailed assessment of intercrystalline heterogeneity is to evaluate grain aspect

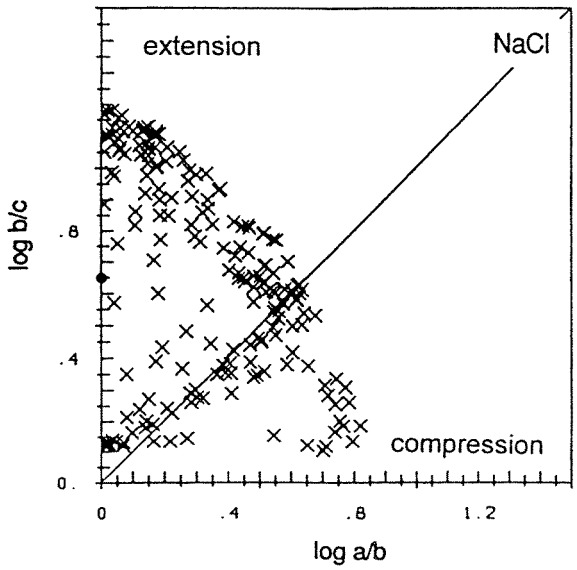

Figure 5. VPSC deformation simulation of halite in extension to 100% equivalent strain. Diagram illustrates the aspect ratios of strain ellipsoid axes of individual grains. Note the wide distribution of shapes. For Taylor all grains plot at $\log a/b = 0$ and $\log b/c = 0.65$. The distance from the origin indicates the degree of deformation. Even though the macroscopic strain prescribes extension (i.e. constriction) many grains deform in the plane strain (diagonal line) and some even in the field of compression (i.e. flattening).

ratios (figure 5). In such diagrams the distance from the origin increases with total deformation and the location determines whether a grain ellipsoid is elongated, flattened or is in plane strain. The macroscopic strain on the aggregate after 100% elongation is indicated by the full circle on the abscissa in figure 5 and for Taylor all grains plot at that location ($\log b/c = 0.65$, $\log a/b = 0$, where the ellipsoid axes are $a < b < c$). Self-consistent predictions show a wide distribution: some grains barely deform at all, others show very large deformation, many have a plane-strain geometry and some are even oblate.

At higher temperature critical shear stresses of all systems are similar and in this case there is no noticeable difference between Taylor and self-consistent simulations. The example of halite reveals some of the unique features of polycrystal plasticity models. The different deformation of individual orientations in the self-consistent model is an important feature to approach systems with a high plastic anisotropy. The model not only predicts the orientation of each grain but also active slip systems, number of active slip systems in a grain, total deformation and shape of deformed grains, all of which can be used to compare experiments with simulations.

4. Calcite and dolomite: curling—strain path during tectonic deformation in the crust

The trigonal (rhombohedral) carbonate minerals calcite $CaCO_3$ and dolomite $(Ca, Mg)CO_3$ have many slip systems, each family with different critical resolved shear stresses. They also deform by mechanical twinning (table 1). Critical shear stresses are well established through experiments on single crystals. They vary particularly as a function of temperature and to a lesser degree of strain rate. As the importance of mechanical twinning diminishes with increasing temperature, the compression texture of calcite changes from a (0001)

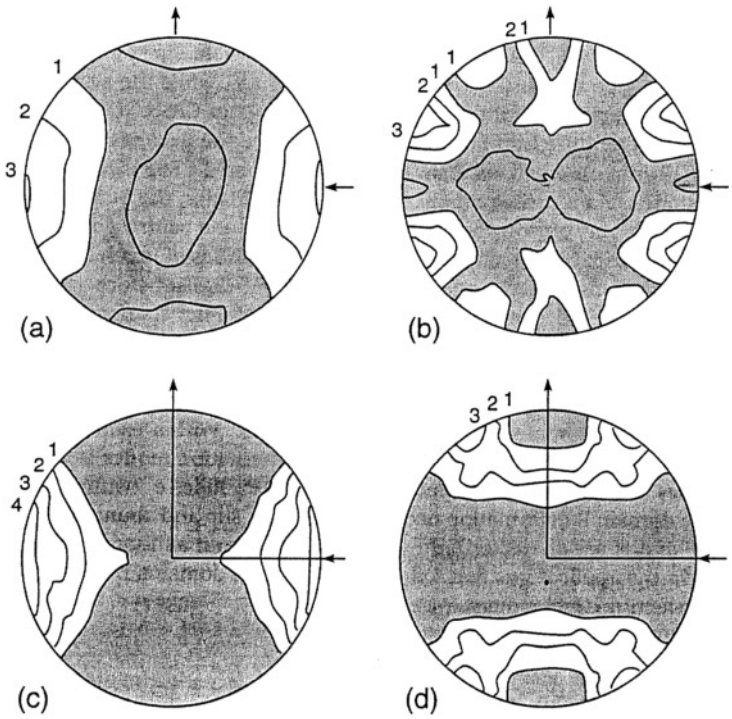

Figure 6. 0001 pole figures for calcite deformed in plane-strain pure shear. Top: experimental pole figures at (a) 100 °C and (b) 400 °C. Bottom: VPSC simulated pole figures for critical shear stresses corresponding to (c) low temperature and (d) high temperature. Equal area projection (Tomé *et al* 1991b).

maximum near the principal shortening direction to a (0001) double maximum (figure 6). These transitions could be reproduced with simulations based on a topology analysis of the single-crystal yield surface for calcite (Tomé *et al* 1991b) and are directly related to changes in critical resolved shear stresses and slip system activity. By changing the critical shear stress of the secondary slip system f^- and that of e^+ twinning relative to the primary slip system r^-, a whole range of different texture types is produced, as illustrated in a topology diagram (figure 7).

For plane-strain deformation of calcite different polycrystal plasticity models (Taylor, relaxed constraints and self-consistent theories) provide rather similar texture results, contrary to halite. This is due to a fairly equiaxed single-crystal yield surface, compared to other minerals and particularly in a subspace that contains most plane-strain paths, with many (21) potentially active slip systems. Simulated texture patterns compare favourably with experiments (Kern 1971, Takeshita *et al* 1987).

For axial compression this is different and Taylor simulations do not agree with experiments. Experimental inverse pole figures show a concentration of compression axes at negative rhombs $\{0h\bar{h}l\}$ with a shoulder towards (0001) (Wenk 1973) (figure 8(a)) whereas Taylor simulations have a concentration at positive rhombs $\{h0\bar{h}l\}$ (figure 8(b)). The experimental pattern for axial compression is qualitatively similar to that obtained experimentally when calcite is deformed in plane-strain compression and the sample is rotated about the compression direction (Wenk *et al* 1986). This is reminiscent of the 'curling' effect during compression of face-centred cubic (fcc) metals and extension of body-centred-

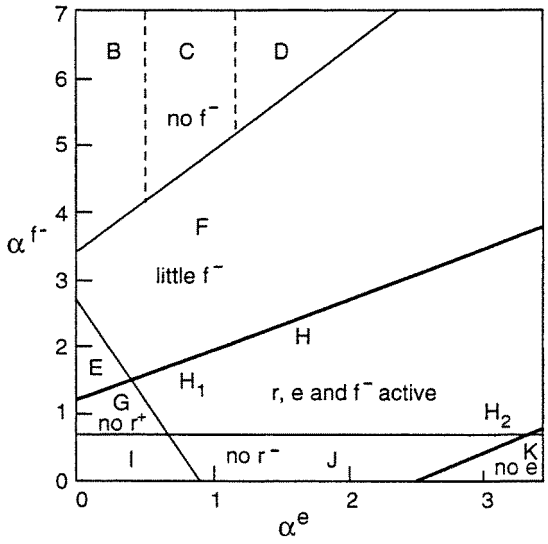

Figure 7. Simplified single crystal yield surface topology diagram for calcite, assuming different critical shear stress ratios (see table 1 for systems). The main topological domains with associated active systems are indicated. The axes are ratios for f- slip and e twinning, assuming that $r^- = 1$ (Takeshita *et al* 1987).

Table 1. Major deformation mechanisms in rhombohedral carbonates. Shear stresses (in MPa) for low temperature (LT, 100 °C) and strain rates of about 10^{-5} s^{-1} interpolated and estimated from table 1 p 362 of Wenk (1985) (see also De Bresser and Spiers (1997)).

	LT	HT
Calcite $CaCO_3$		
Slip:		
$r^- = \{10\bar{1}4\}\langle 20\bar{2}1\rangle$	50	15
$r^+ = \{10\bar{1}4\}\langle \bar{2}021\rangle$	80	15
$f^- = \{\bar{1}012\}\langle 0\bar{2}21\rangle\langle \bar{2}201\rangle$	150	30
$f^+ = \{\bar{1}012\}\langle 02\bar{2}1\rangle\langle 2\bar{2}01\rangle$	200	50
$f = \{\bar{1}012\}\langle 10\bar{1}1\rangle$	—	30
$c = (0001)\langle 2\bar{1}\bar{1}0\rangle$	–	20
Twinning:		
$e^+ = \{\bar{1}018\}\langle 40\bar{4}1\rangle$ $\gamma = 0.69$	10	7
Dolomite $(Mg, Ca)CO_3$		
Slip:		
$c = (0001)\langle 2\bar{1}\bar{1}0\rangle$	50	130
$f^- = \{\bar{1}012\}\langle 0\bar{2}2\bar{1}\rangle\langle -220\bar{1}\rangle$	170	100
$f^+ = \{\bar{1}012\}\langle 02\bar{2}1\rangle\langle 2\bar{2}01\rangle$	250	150
$r^- = \{10\bar{1}4\}\langle \bar{1}2\bar{1}0\rangle$	250	150
Twinning:		
$f^- = \{\bar{1}012\}\langle 10\bar{1}1\rangle$ $\gamma = 0.59$	90	100

cubic (bcc) metals where individual crystals deform locally in plane strain even though the macroscopic deformation is axisymmetric (Hosford 1964). Grain curling is automatically accounted for in self-consistent model calculations, without the need to impose explicit conditions (Lebensohn *et al* 1998) (figure 8(c)). The Taylor model predicts axial compression

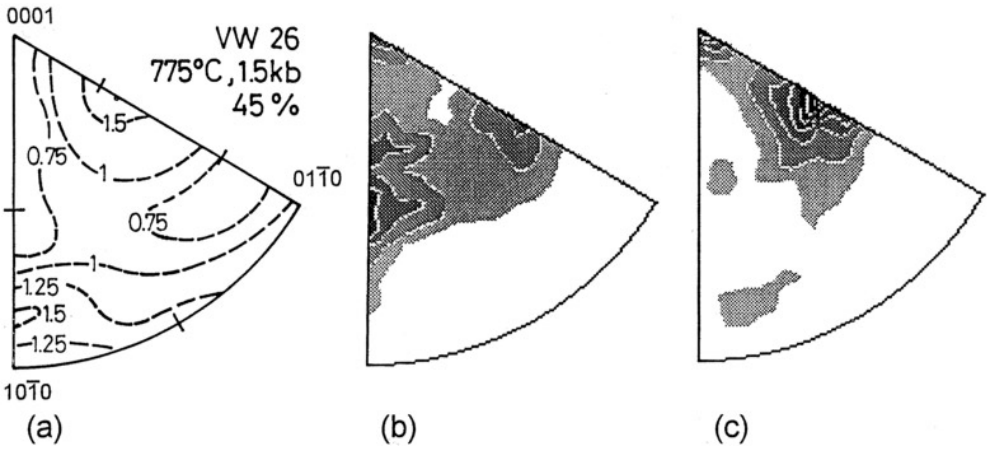

Figure 8. Inverse pole figures showing textures of calcite deformed in axial compression. (a) Axial compression experiment (Wenk *et al* 1993), (b) Taylor simulations for axial compression, (c) VPSC simulation. Equal-area projection, pole densities in (b), (c) above 1 m.r.d. are shaded (Lebensohn *et al* 1998).

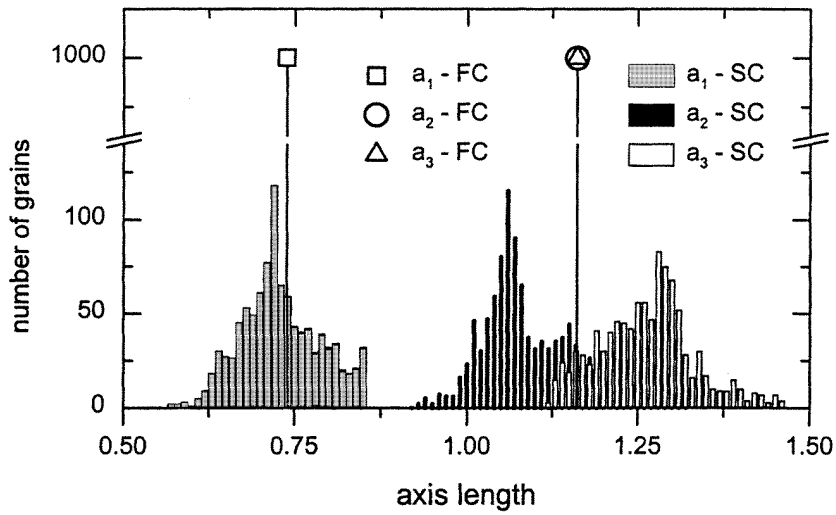

Figure 9. Simulated grain shape distribution for calcite deformed in axial compression to 30% strain. Original axis length is one. The Taylor model predicts a pancake shape whereas VPSC predicts a bimodal distribution approaching plane strain (Lebensohn *et al* 1998).

grains with a uniform pancake shape. VPSC provides a distribution with more and less deformed grains. In addition this distribution is for the long axes bimodal, consistent with plane-strain geometry (figure 9).

In halite and calcite the self-consistent model has been useful in improving texture predictions. Compared with the Taylor model, self-consistent simulations provide different rotations, based on different activity of slip systems. In most cases texture analyses rely on bulk measurements and there is no information about the actual activity of slip systems related to orientation. Slip systems in deformed dolomite (Ca, Mg)CO_3 polycrystals have been investigated with transmission electron microscopy (Barber *et al* 1994). It was confirmed by TEM analysis that those systems predicted to be dominantly active for a given orientation are

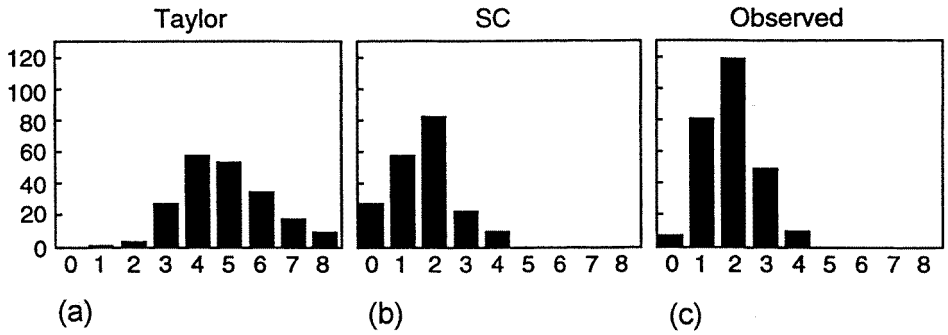

Figure 10. Deformation of polycrystalline dolomite. Histograms represent the number of significantly active slip systems per grain. (a) Predictions based on the viscoplastic Taylor theory, counting systems that contribute 10% or more to the total shear, (b) predictions based on VPSC, (c) slip systems actually observed by TEM investigations of experimentally deformed dolomite (Barber *et al* 1994).

actually present. Also it was found that the average number of significantly active slip systems (contributing 10% or more to the total shear) is about two, in good accord with self-consistent predictions and much lower than 4–5 as required by Taylor theory (figure 10).

For structural geologists often the detailed strain history is of concern in the interpretation of deformation of mountain belts in the crust. Textures are significant because they are often sensitive to the path. For example, a geologist needs to determine if a tectonic zone has been subject to non-coaxial shearing in a shear zone (figure 11, bottom) or coaxial crustal thinning (figure 11, top). Both paths can lead to an identical finite strain. Naturally deformed calcite rocks, limestones and marbles, often display strong preferred orientation. Texture patterns of calcite in deformed marbles have been used to determine the partitioning of deformation into a coaxial deformation component and a non-coaxial (simple shear) component and to infer the deformation history. One of the universal principles of texture interpretation is symmetry and it has been widely applied in geological situations: the texture symmetry cannot be lower than the symmetry of the strain path, if it started out uniform (Paterson and Weiss 1961). For coaxial deformation one expects orthorhombic pole figures, whereas a non-coaxial path is likely to produce monoclinic pole figures.

In nature there are mixed paths between simple shear and pure shear, still in plane strain, to arrive at the same deformation. We can define $\tan \eta = \gamma/2\varepsilon$ as the ratio of simple shear with respect to pure shear and geologists refer to it as the 'strain partitioning factor' (Wenk 1998). The partitioning factor can be obtained by comparing natural textures with those obtained from polycrystal plasticity models. Calculated 0001 pole figures for plane strain document a symmetrical (orthorhombic) pure shear pole figure and an asymmetrical (monoclinic) simple shear pole figure and intermediate states (figure 12). The relative amount of simple shear can be quantified by measuring the angle of asymmetry ω (defined in figure 13(d)) between the (0001) maximum and the shear-plane normal. From polycrystal plasticity calculations one can construct an empirical determinative diagram to assess the amount of simple shear from the asymmetry of the (0001) texture maximum (Wenk *et al* 1987) (figure 13(a)).

In practice, geologists collect oriented rock samples in the field, then measure pole figures in the laboratory relative to geological coordinates, such as schistosity plane and lineation direction which define the shear plane and shear direction. From the asymmetry ω of the 0001 pole figure maximum relative to the shear plane the sense of shear can be inferred. From the angle of asymmetry and using the determinative diagram in figure 13(a), the strain

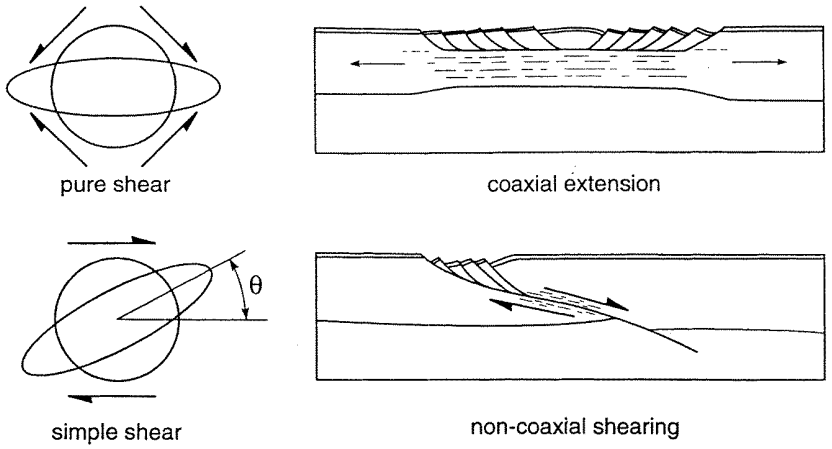

Figure 11. Cartoon comparing crustal deformation by coaxial thinning (top) and non-coaxial shearing (bottom). Coaxial thinning may occur by pure shear, whereas non-coaxial shearing occurs by simple shear. The finite-strain (shape of ellipse) may be the same but in simple shear the ellipse is inclined by an angle θ to the shear plane (Wenk *et al* 1987).

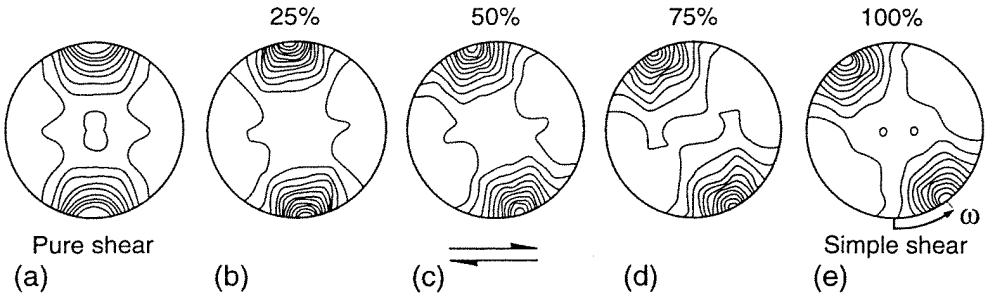

Figure 12. 0001 pole figures of calcite obtained with the Taylor model for 100% equivalent strain. Pure shear on the left, mixed modes in the centre and simple shear on the right (Wenk *et al* 1987). Note the increasing asymmetry ω of the [0001] maximum relative to the shear plane (horizontal). The sense of shear is indicated.

partitioning can be estimated. Whereas many marbles in core complexes of the Western United States show almost symmetrical patterns of (0001) axes (Erskine *et al* 1993) (figure 13(b)) and presumably formed during crustal extension of the Basin and Range province, limestones from the spreading nappes in the Alps have generally highly asymmetric texture patterns attributed to shearing on thrust planes (Dietrich and Song 1984, Ratschbacher *et al* 1991) (figure 13(c)). In Alpine spreading nappes the component of simple shear ranges from 0 to 100%. While metallurgists mostly use plasticity theory to predict future behaviour, geologists have applied it to reconstruct the past history.

5. Quartz: strain-rate sensitivity and recrystallization

Both Taylor (1938) and Sachs (1928) assumed a rigid-plastic behaviour; implying that no deformation (i.e. dislocation movement) occurs until the critical resolved shear stress is reached, at which point deformation is instantaneous. At intermediate and high temperatures where lattice diffusion and climb become active, it is likely that crystals deform even at

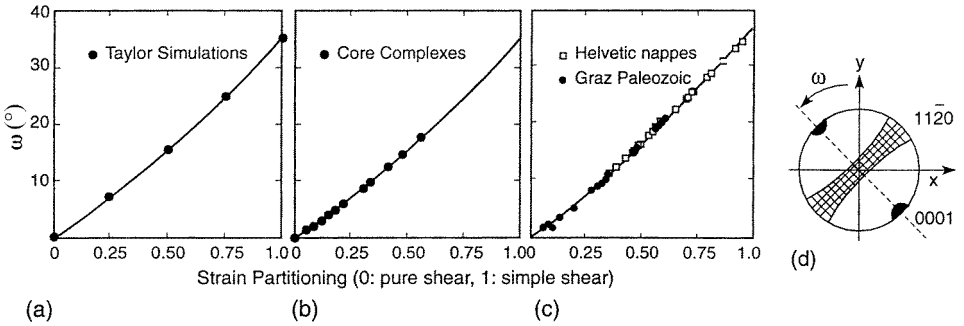

Figure 13. (a) Determinative diagram with angle of asymmetry ω against the strain partitioning factor (percentage of simple shear deformation) as obtained from Taylor simulations (figure 12). Results for (b) marble mylonites from core complexes of the American Cordillera (Erskine *et al* 1993) and (c) various limestone textures from Alpine spreading nappes (Ratschbacher *et al* 1991). (d) Definition of the diagnostic angle ω.

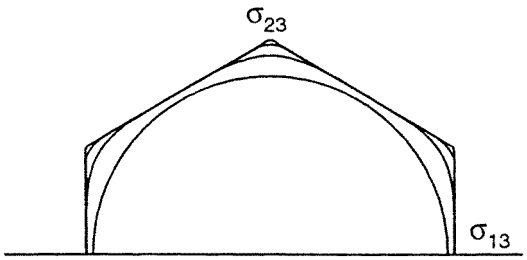

Figure 14. Two-dimensional sections through the single-crystal yield surface of quartz for stress exponents 3, 9 and 99. Stress coordinates σ_{23}–σ_{13} are indicated (Wenk *et al* 1989a).

low stresses, albeit more slowly. Metallurgists have originally introduced a viscoplastic power law description as a way to deal with the choice of slip system combinations at vertices of the single-crystal yield surface in cubic metals where ambiguities exist in the rigid-plastic case (Asaro and Needleman 1985). In low-symmetry minerals this ambiguity is generally of no concern but the strain-rate sensitivity is much higher and has an influence on textures. Minerals are somewhere intermediate between a Newtonian viscous behaviour ($n = 1$) where the strain rate is proportional to the stress and a rigid plastic behaviour ($n = \infty$). For trigonal quartz, SiO_2, with a low-stress exponent of three (high strain-rate sensitivity of $1/3$) the single-crystal yield surface is highly rounded (figure 14) and strain is distributed more uniformly over many systems, causing a reduction in anisotropy. The viscoplastic quartz textures, displayed as 0001 pole figures (figure 15(b), (c), are smoother than the rigid plastic texture (figure 15(a)), corresponding better to some natural quartz textures such as that in the first published fabric diagram (figure 15(d)) (Schmidt 1925).

There have been several studies of the orientation-dependent grain shape distribution for quartz. In quartzites one observes often highly deformed and relatively undeformed grains adjacent to each other in the same sample. Bouchez (1977) recorded grain aspect ratios in addition to orientation and noticed that *c*-axes of weakly deformed grains are at high angles to Y (figure 16(a)), whereas strongly deformed grains cluster around the intermediate fabric direction Y (in the schistosity plane and normal to the lineation, in the centre of the pole figure) (figure 16(b)). This has since then been observed in many cases. If texture development of

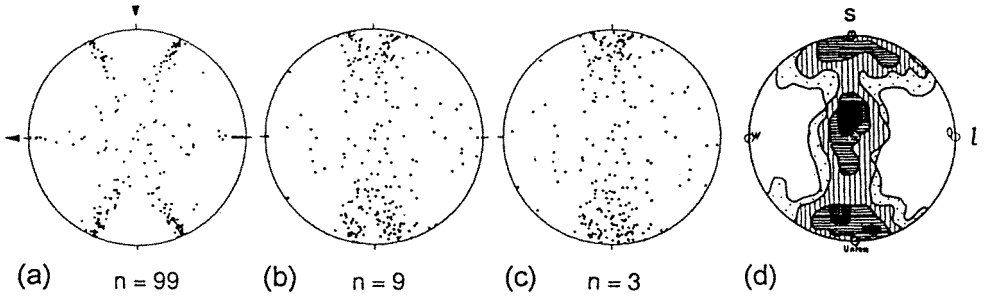

Figure 15. (a)–(c) Taylor simulations for quartz in pure shear illustrating the effect of the stress exponent (inverse of the strain-rate sensitivity) (Wenk *et al* 1989a). The stress exponent $n = 3$ (in $\dot{\gamma} = \tau^n$), which is applicable to quartz, gives the most realistic texture and compares well with the first measured quartz texture on the right-hand side (d) (Schmidt 1925) (compression and extension directions are indicated by arrows, s is the normal to the schistosity and l is the lineation).

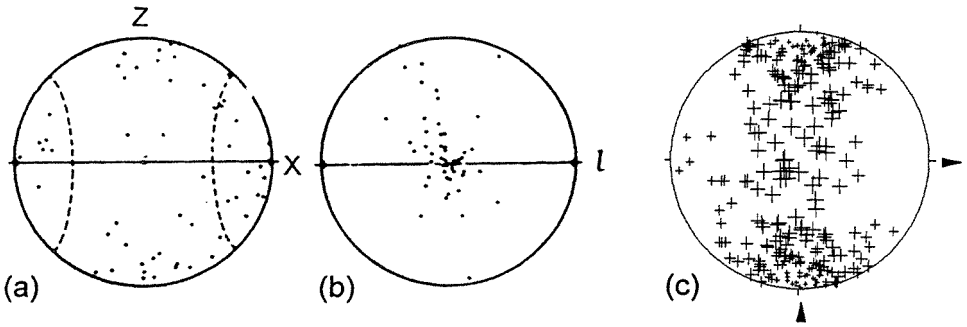

Figure 16. 0001 pole figures of quartz. (a) Naturally deformed quartzite, foliation horizontal and lineation l to the right (fabric coordinates X and Z, used in the geological literature are indicated, Y is in the centre). Collection of grains with an aspect ratio <4 (weakly deformed grains). (b) Same sample as (a) but a collection of strongly deformed grains with an aspect ratio >8 (Bouchez 1977). (c) Viscoplastic self-consistent simulations of pure shear deformation. Symbol sizes are proportional to strain (Wenk *et al* 1989a). Arrows indicate the compression and extension direction, respectively.

quartz is modelled with the self-consistent theory for pure shear conditions, highly deformed grains are indeed predicted in the intermediate strain direction, as indicated by the large symbols in figure 16(c).

Quartz is one of the most important rock forming minerals in the crust and all aspects of preferred orientation and microstructure have been studied extensively (see Wenk 1994). In many rocks quartz is partially or completely recrystallized and this ought to be incorporated into deformation models that simulate texture evolution. In some cases recrystallized textures are similar to deformation textures, in other cases they are very different. In quartzites deformed at high temperature it was noticed that the recrystallization texture emphasized those orientations for which the self-consistent method predicted large deformation (figure 16(c)). This was the motivation for exploring dynamic recrystallization based on an analysis of the deformation behaviour and the self-consistent polycrystal plasticity theory lends itself well as a foundation for modelling dynamic recrystallization because it predicts different deformations for differently oriented grains (Wenk *et al* 1997).

A driving force for recrystallization is the strain energy stored in individual grains. Highly

deformed grains (or highly deformed regions within a grain) have a tendency to nucleate new grains, given the availability of significant misorientations, and those with a low stored energy have a tendency to grow at the expense of their neighbours. The stored energy is introduced by accumulations of dislocations. Depending on the respective importance of nucleation and boundary migration processes, the recrystallization textures are expected to favour either highly deformed texture components or less deformed components.

Deformation simulations with the self-consistent model provide a population of grains with a variation in deformation and correspondingly in stability. The microstructural hardening of slip systems during deformation adds dislocations, and thus strain energy, to grains after each deformation step. Grains with a high stored energy are likely to be invaded by their neighbours with a lower stored energy. If the stored energy of a grain is lower than the average, it grows; if it is higher, it shrinks. The grain-boundary velocity is assumed to be proportional to the difference in stored energy. A grain may disappear.

For so-called 'nucleation' microstructural heterogeneities are most influential. These heterogeneities are generally linked to strain. In the model the nucleation rate depends on the individual strain rate. Nucleation is only allowed to take place if the deformation is above a certain threshold corresponding to the requirement for high-angle subgrain boundaries which become sufficiently mobile. For simplicity and for lack of other information it is assumed that the new crystal is in the same orientation as the old one, but the stored energy of the new crystal is set equal to zero by returning to the initial critical resolved shear stress, and the grain is restored to an equiaxed shape.

During dynamic recrystallization all grains are evaluated after each deformation step and allowed to grow, shrink or nucleate and the characteristics (deformation, size, orientation, shape, slip systems) of all grains are updated. The development of the microstructure and texture is determined by the balance between nucleation and growth. These processes are described in the model by only three parameters: a mobility parameter, a nucleation parameter and a nucleation threshold.

In recrystallized natural quartz textures there is an enigmatic (0001) maximum in the intermediate strain direction (figure 15(d) and 17(a)) that cannot be explained by deformation. In pure shear simulations a broad maximum near the shortening axis (vertical) develops (figure 16(c)). There are only a few grains in the intermediate strain direction (centre of pole figure) but they are highly deformed compared to those at the periphery. During dynamic recrystallization grains near the centre are nucleating (symbol $\times$) and become strain-free, retaining their old orientation. They grow and may nucleate again (symbol size is proportional to grain size); those near the periphery, though less deformed, are consumed by the newly nucleated grains (figure 17(b), (c)) in reasonable agreement with textures in natural quartzites (figure 17(a)).

A particularly interesting application of the self-consistent recrystallization model has been to a quartzite, naturally deformed in simple shear and dynamically recrystallized (Takeshita *et al* 1999). In this sample the texture consists largely of four orientation components. Two (0001) maxima, A and B are at high angles to the shear plane ('foliation plane') and displaced *against* and *with* the sense of shear, respectively (figure 18(a)). A third component C is in the intermediate strain direction (centre of pole figure) and the fourth component D is subparallel to the shear direction. Simulations indicate that B grains are favourably oriented for basal (0001) slip and highly deformed, C grains are oriented for prismatic slip $\{10\bar{1}0\}\langle 2\bar{1}\bar{1}0\rangle$ and also strongly deformed (figure 18(b)). A grains have undergone little deformation and D grains are moderately deformed. The degree of recrystallization increases with strain in the sequence A $<$ D $<$ B $<$ C. These predictions agree with observations made with the optical microscope that identify texture, active slip systems, grain aspect ratios and evidence

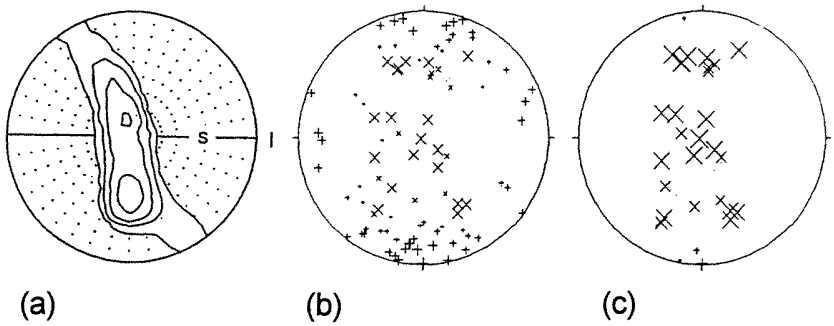

Figure 17. 0001 pole figures for quartz. (a) Typical texture of a naturally recrystallized quartzite with a (0001) maximum in the 'intermediate' fabric direction, normal to the lineation *l* and in the plane of schistosity *s*. (b), (c) Pure shear VPSC simulation of dynamic recrystallization after eight deformation steps. (b) Texture after 10 steps, (c) texture after 14 steps. Grains with diagonal crosses ($\times$) have nucleated, those with parallel crosses (+) have not. The symbol size is proportional to the grain size which changes due to boundary migration (Wenk *et al* 1997).

of boundary mobility. The final recrystallization texture of quartz displays an (0001) maximum displaced *with* the sense of shear (B), contrary to the deformation texture but in agreement with independent geological evidence in many deformed quartzites (Law 1990). Simple shear experiments produce similar texture patterns with a (0001) maximum displaced *against* the sense of shear during deformation and one with the maximum displaced *with* the sense of shear during recrystallization (Dell'Angelo and Tullis 1989).

The self-consistent model that includes dynamic recrystallization has been successful in explaining recrystallization textures in many mineral systems such as halite (Wenk *et al* 1997), calcite deformed in compression (Lebensohn *et al* 1998), calcite deformed in simple shear (Kunze *et al* 1998), olivine deformed in simple shear (Wenk and Tomé 1999) and ice (Wenk *et al* 1997).

6. Granite: deformation of polyphase aggregates

If models allow heterogeneous (intragranular) deformation, incompatibility between grains has to be accommodated somehow and this cannot be done within a context that assumes grains to deform homogeneously. An attempt has been made to model a system with high plastic anisotropy, causing large intragranular heterogeneity, a composite of quartz and rigid mica particles (Canova *et al* 1992), by introducing microstructure in the self-consistent model and dividing each grain into domains (small cubes). Each cubic domain deforms according to its 26 nearest-neighbour cubes. It was possible to simulate gradients in strain rate and stress in single grains, and variations depend on the neighbourhood (figure 19). With this '*n*-site VBSP approach' predicted quartz textures of a single-phase quartzite are stronger than those for a quartzite with suspended rigid particles which agrees with experiments (Tullis and Wenk 1994). The quartz-mica aggregate shows a higher dispersion of intracrystalline strain rates around rigid inclusions.

7. Olivine: seismic anisotropy in the Earth's mantle

The orthorhombic silicate mineral olivine Mg_2SiO_4, which is the main constituent of the upper mantle of the Earth, has only a few potential slip systems: (010)[100], (001)[100]

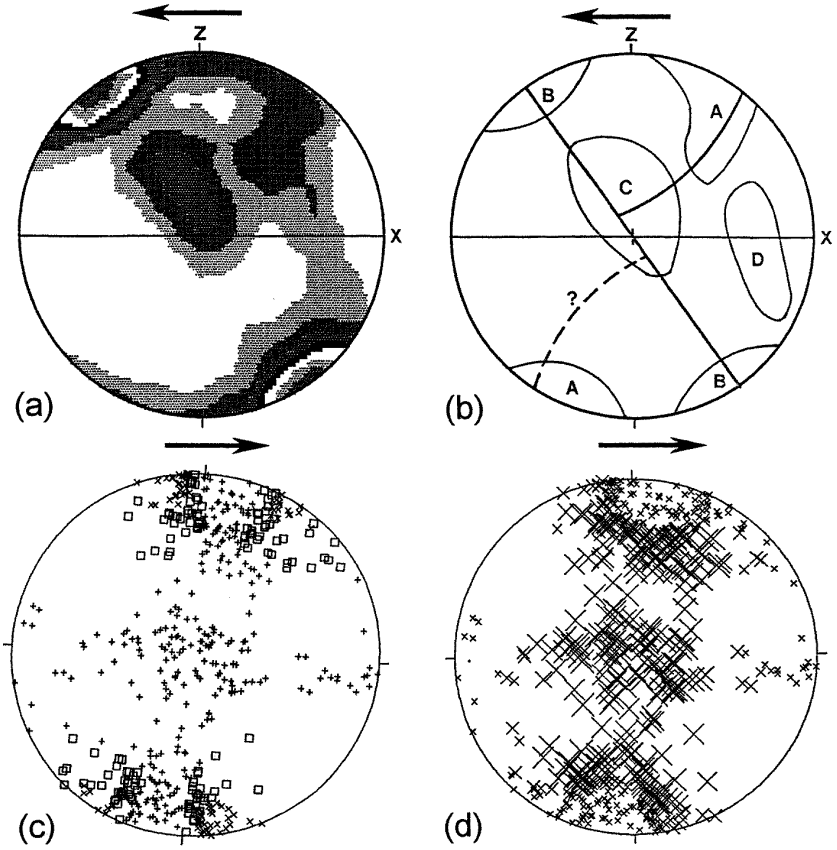

Figure 18. 0001 pole figures for quartz. (a) Metamorphic quartzite deformed in simple shear, (b) schematic diagram illustrating the four main orientation components, (c) VPSC simulations of simple shear deformation with symbols indicative of dominant slip systems ($\times$ basal slip, + prismatic slip, equal activity of basal and prismatic slip). (d) VPSC simulation of dynamic recrystallization with preferred grain growth after nucleation, symbol size corresponds to the grain size (Takeshita *et al* 1999).

and (100)[001]. The slip systems are not sufficient to deform a crystal to an arbitrary shape and therefore the strict Taylor model requiring uniform deformation of all grains cannot be applied. Normal strain components cannot be accommodated by existing slip systems. The VPSC theory in various forms (Takeshita *et al* 1990, Wenk *et al* 1991, Tommasi *et al* 1997), a lower bounds approach (Chastel *et al* 1993) and a hybrid formulation (Parks and Ahzi 1990) have been used to model texture development of olivine. All models yielded similar results: in compression one finds an alignment of [100] axes at high angles to the compression direction, in agreement with axial compression experiments (Avé Lallemant and Carter 1970, Nicolas *et al* 1973) and a [100] maximum inclined to the shear direction, as observed in simple shear experiments (Zhang and Karato 1995).

In recent years seismic anisotropy in the upper mantle of the Earth has received much attention (e.g. Nishimura and Forsyth 1989, Silver 1996). Anisotropy of seismic velocities in rocks can have various sources which may be due to a layered arrangement of components or due to crystallographic preferred orientation. The presence of oriented microfractures, the presence of partial melt and to a lesser extent the grain shape are also influential. Velocities

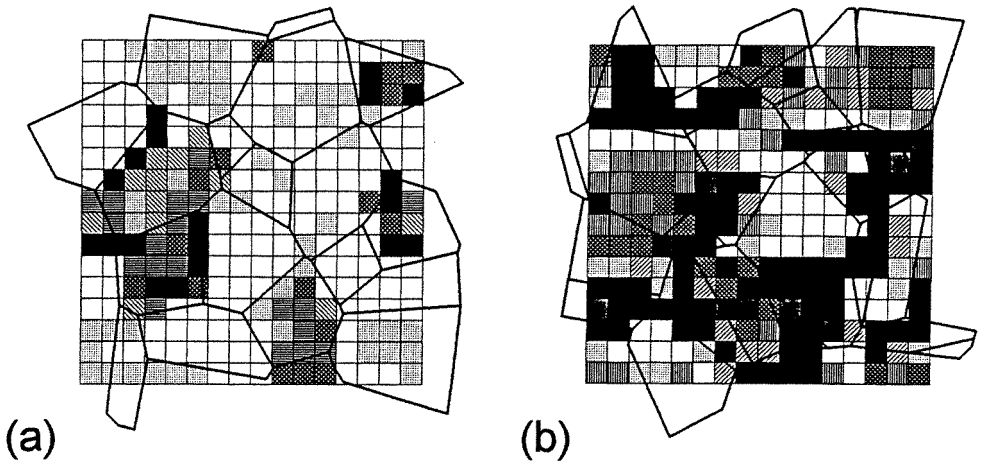

Figure 19. Aggregate of (a) pure quartz and (b) a quartz-mica mixture deformed with the VPSC *n*-site model that divides space into small cubes. After 50% axial compression stress gradients develop that are particularly large for the aggregate with rigid mica particles (b). The microscopic compressive stress component is illustrated with shades (Canova *et al* 1992).

through a rock with oriented fractures are much higher parallel to the fractures than across them (Crampin 1981). With increasing pressure microfractures close and their influence on anisotropy diminishes. Kern and Wenk (1990) measured in phyllosilicate-rich rocks at 50 MPa a velocity anisotropy of 19%, due to both crystal alignment and oriented microfractures. Above 500 MPa, where microfractures are largely closed, the anisotropy is reduced to 12% and is only due to the crystallographic preferred orientation.

Olivine crystals exhibit about a 25% difference in longitudinal (p) velocities between the slowest [010] and the fastest crystal directions [100]. Therefore, in an aggregate with preferred orientation of component crystals one also expects a directional dependence of seismic wave propagation. In the mantle large cells of convection are induced by instabilities and driven by temperature gradients (e.g. Hager and O'Connell 1981) and it is of interest to model texture development during convection because deformation of the upper mantle is directly expressed in processes in the Earth's crust, such as plate tectonics, sea floor spreading, volcanic activity, earthquakes and mountain building.

On a microscopic scale, olivine is deformed by intracrystalline processes, slip of dislocations in the crystal lattice and accompanying dynamic recrystallization. A convection cell in the Earth is a very large heterogeneous system. In order to correctly predict the flow behaviour at any point in the mantle, we need to consider the microscopic deformation processes in all single crystals over the whole macroscopic deformation history. Micro–macro linking problems fascinated Gilles Canova and he was just ready to start an investigation of olivine dislocation dynamics to provide a solid basis for macroscopic deformation modelling in the Earth when he passed away.

On a larger scale Chastel *et al* (1993) and Dawson and Wenk (1999) have used a finite element model based on crystal plasticity to predict texture development in a large heterogeneous convection cell extending over thousands of kilometres. Buoyancy, associated with temperature gradients, drives the convective flow within the cell. The equations that govern such a large system include conservation of energy, balance of linear momentum, kinematic requirements for compatibility, relations between stress and deformation from polycrystal plasticity and boundary conditions. These equations are solved with the

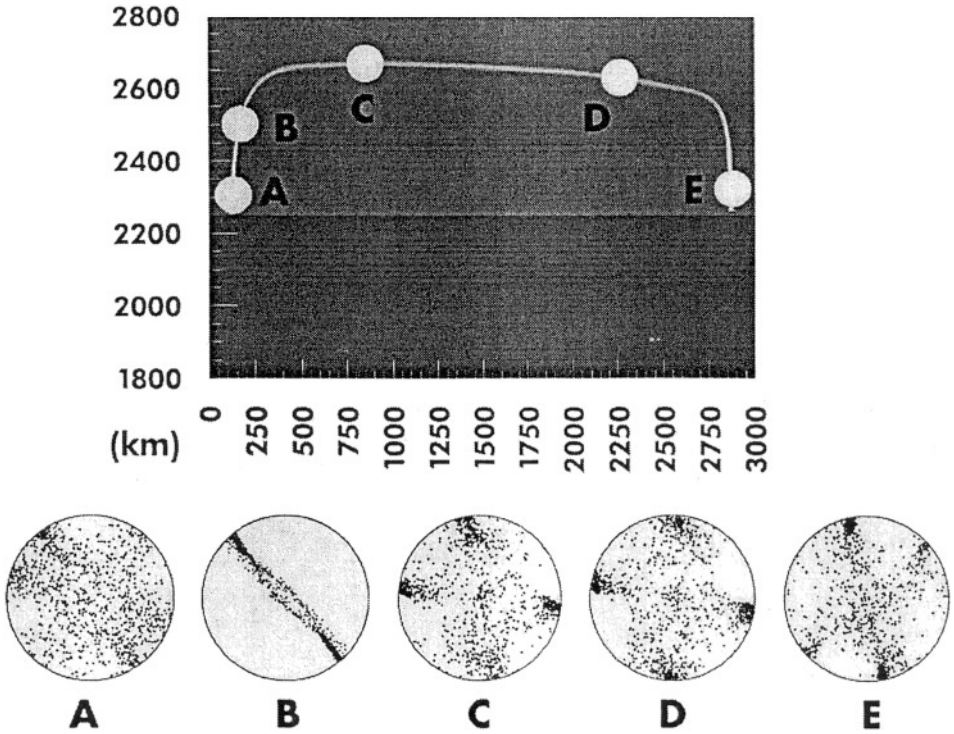

Figure 20. Simulated texture development during convective flow in the upper mantle. Evolution of texture along a streamline from A to E, represented by olivine [100] pole figures (1000 grains). During upwelling (left) a strong texture develops and changes (Dawson and Wenk 1999).

finite-element method which gives approximate solutions for the velocity and temperature distribution. Figure 20 follows texture development in the upper mantle along a streamline in pole figures of olivine [100] axes. During upwelling a strong texture develops very rapidly (B). The preferred orientation stabilizes during spreading (C,D) and attenuates during subduction (E). The pole figures are distinctly asymmetric due to the component of simple shear. While the finite-strain along a streamline increases monotonically, the texture does not. Neither does it completely revert to randomness as the aggregate reenters the lower layer (E). Texture development during convection is a highly dynamic process which is best illustrated in an animated video (Wenk *et al* 1999b). It has been surprising to find great heterogeneity, with some regions highly textured and others almost isotropic.

Knowing the orientation of crystallites in a convection cell and the elastic properties of single crystals, one can then average over sectors of the cell to get seismic velocities in different directions. The variations of the p-wave velocities in this simulated textured mantle predict a similar azimuthal anisotropy (figure 21(a)) as that derived from seismic data (Morris *et al* 1969) (figure 21(b)). Seismologists noticed that seismic waves travel about 5% faster perpendicular to oceanic ridges than parallel to the ridges. In Hess (1964) this was interpreted as a result of a preferential alignment of crystals with directional properties, and it was proposed that this alignment was attained during the convection process.

From such models it is evident that the mantle is not a structureless viscous medium but shares many properties with a single crystal which displays internal structure and anisotropy. The approach described links processes that occur within crystals on an atomic scale to

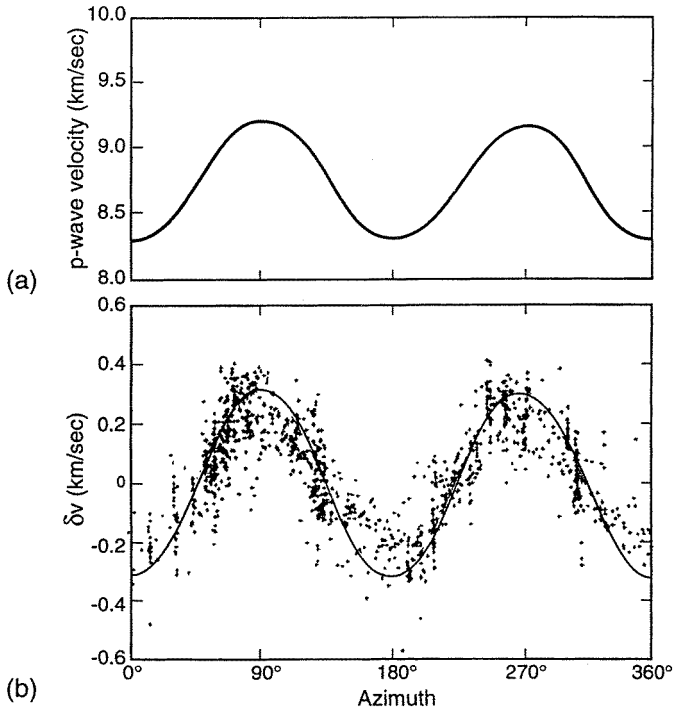

Figure 21. Azimuthal variation of seismic longitudinal wave velocities (in km s^{-1}); (a) obtained by averaging the upper 50 km of the mantle based on texture predictions with an anisotropic convection model (Chastel *et al* 1993), (b) observed *p*-wave velocities in the vicinity of Hawaii (0° is N, 90° is E) (Morris *et al* 1969).

macroscopic dimensions of the size of continents. By including polycrystal plasticity, geophysical deformation modelling is entering a new state of refinement and future convection modelling should include the complexities of anisotropy and mechanical properties.

However, in the upper mantle deformation by dislocation glide is accompanied by dynamic recrystallization. Experiments by Zhang and Karato (1995) have shown that in simple shear deformation at low strains an asymmetric texture develops ([100] rotated away from the shear direction against the sense of shear), whereas at large strain where recrystallization is pervasive, the pattern is symmetrical ([100] parallel to the shear direction). Again we turn to the VPSC theory with the extension for dynamic recrystallization described before. For deformation the model predicts the asymmetric [100] maximum observed in experiments (figure 22, left). During dynamic recrystallization, first a bimodal orientation distribution develops with one maximum parallel to the shear direction and a second one at high angles (figure 22, 35 steps). With continuing recrystallization the first maximum becomes dominant and is stable to very large strains (figure 22, 75 steps). This texture component corresponds to an 'easy slip' orientation for which the microscopic slip direction of the dominant slip system [100] is parallel to the macroscopic shear direction and the microscopic slip plane (010) parallel to the shear plane (Wenk and Tomé 1999).

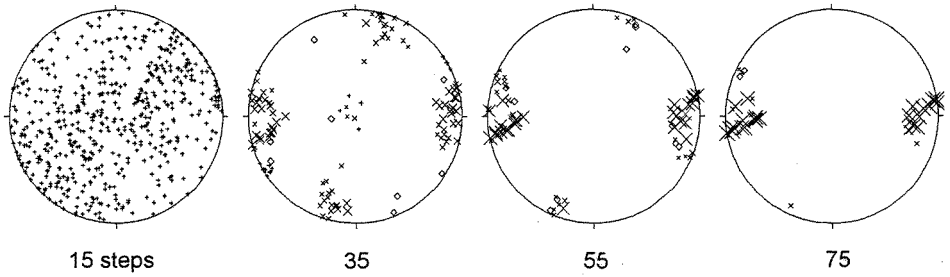

Figure 22. Olivine [100] pole figures illustrating VPSC simulation of texture evolution during dynamic recrystallization in simple shear. Recrystallization is initiated after 20 steps, each step corresponds to an equivalent strain of 2%. Shear plane is horizontal, sense of shear is dextral. + grains have not nucleated, × are nucleated grains and diamonds (◊) are grains that have disappeared during the last step (Wenk and Tomé 1999).

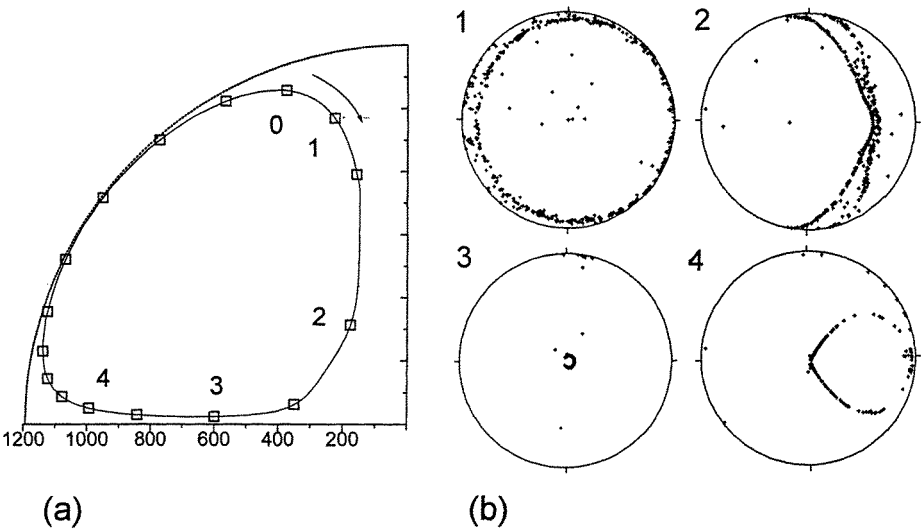

Figure 23. FEM model of second-order harmonic convection in the Earth's core. A streamline is shown with subduction at the poles and extrusion in the equatorial plane. At step 0 the texture is random. 0001 pole figures for ε-iron are shown for four locations along the streamline (Wenk *et al* 1999a).

8. ε-iron: anisotropy in the inner core

The core of the Earth is largely composed of iron. The outer core is liquid but the inner core is crystalline. It is likely that the prevalent phase is hexagonal (ε) iron with the same structure as other hexagonal metals. Texture development in those has been investigated in detail with the self-consistent model (e.g. Lebensohn and Tomé 1993, 1994, Lebensohn *et al* 1994, 1996, Tomé and Canova 1998).

Seismological evidence suggests that also the inner core is anisotropic (Woodhouse *et al* 1986, Vinnik *et al* 1994). Waves travel faster along the NS axis than in the equatorial plane. There are various ways to develop anisotropy. One mechanism is preferential growth. However, for most larger systems, extending over hundreds of kilometres, a more likely mechanism is deformation during convection in a spherical system, in a similar way as in

the upper mantle, except that in the mantle convection is induced by a temperature gradient, whereas in the core it is due to internal heating. If second-harmonic degree convection is modelled with finite-element codes, the strain history along flow lines can be used to simulate development of crystallographic preferred orientation. It is assumed that the deforming phase is ε-iron and that slip systems are similar to those of hcp titanium (basal and prismatic slip active). Indeed preferred orientation does develop rapidly (figure 23). From the orientation patterns and taking elastic properties for ε-iron at core pressure, the elastic properties of the aggregate can be calculated. Preliminary calculations suggest that the observed seismic anisotropy is consistent with crystal alignment during a convection process (Wenk *et al* 1999a).

9. Conclusions

Having arrived at the centre of the Earth the voyage is finished. The preceding discussion illustrated the importance of materials modelling for the understanding of deformation processes in the Earth. It also highlighted the significance of the VPSC theory conceived by Gilles Canova and his colleagues for understanding deformation of materials with a high plastic anisotropy, caused by a limited number of slip systems and low-crystal symmetry. Extending the model to include recrystallization and to treat non-uniform strain paths makes it applicable to model deformation in large heterogeneous systems for a wide variety of conditions.

Looking back it also becomes apparent that the mineralogical examples have been crucial in advancing the self-consistent model and generalizing it for complexities that were encountered in the course of these investigations. Each system displayed different characteristics and documented the wide range of diagnostic information included in VPSC simulations, such as textures, grain size and shape and active slip systems that can be used to ascertain if the model is applicable.

This paper should not give the impression that the self-consistent model is a universal theory to satisfy all aspects of polycrystal plasticity. Like all models it is limited to a certain range of conditions and needs to be re-evaluated whenever the conditions change, or if it is applied to a new system. For some results it will be necessary to use the much more elaborate and computer intense finite-element method (Dawson and Beaudoin 1998) but much information can still be obtained with VPSC. It should also be emphasized that this model constantly evolves to a better balance between equilibrium and compatibility (Molinari and T'oth 1994) or allowing for intracrystalline heterogeneity by invoking an n-site formulation.

Acknowledgments

The author is deeply indebted to Gilles Ganova for helping him towards a better understanding of deformation processes, by his inspiration, kindness and patience. The time which we spent together in France and Berkeley remain highlights. On the occasion of the 'Mecking Fest' in 1997 several participants suggested that I write a summary on polycrystal plasticity in earth sciences for engineers and this seemed to be the perfect opportunity. Much of this work could not have been accomplished without Fred Kocks and the stimulating atmosphere he created at the Center for Materials Science in Los Alamos. The work was supported by the France-Berkeley Fund, NSF, IGPP-LLNL and IGPP-LANL.

References

* Indicates that the publication uses the viscoplastic self-consistent theory of polycrystal plasticity

Alley R B 1988 Fabrics in polar ice sheets: development and prediction *Science* **240** 493–5
Asaro R J and Needleman A 1985 Texture development and strain hardening in rate dependent polycrystals *Acta Metall.* **33** 923–53
Avé Lallemant H and Carter N L 1970 Syntectonic recrystallization of olivine and modes of flow in the upper mantle *Geol. Soc. Am. Bull.* **81** 2203–20
Azuma N and Higashi A 1985 Formation processes of ice fabric pattern in ice sheets *Anal. Glaciol.* **6** 130–4
*Barber D J, Wenk H-R and Heard H C 1994 The plastic deformation of polycrystalline dolomite: comparison of experimental results with theoretical predictions *Mater. Sci. Eng.* A **175** 83–104
*Bennett K, Wenk H-R, Durham W B and Stern L A 1997 Preferred crystallographic orientation in the ice I → II transformation and the flow of ice II *Phil. Mag.* A **76** 413–35
Bouchez J L 1977 Plastic deformation of quartzites at low temperature in an area of natural strain gradient *Tectonophys.* **39** 25–50
Bouchez J L and Duval P 1982 The fabric of polycrystalline ice deformed in simple shear: experiments in torsion, natural deformation and geometrical interpretation *Texture Microstruct.* **5** 171–90
*Canova G R, Wenk H-R and Molinari A 1992 Deformation modelling of multi-phase polycrystals: case of a quartz–mica aggregate *Acta Metall. Mater.* **40** 1519–30
Carter N L and Heard H C 1970 Temperature and rate dependent deformation of halite *Am. J. Sci.* **269** 193–249
*Castelnau O, Canova G R, Lebensohn R A and Duval P 1997 Modelling viscoplastic behaviour of anisotropic polycrystalline ice with a self-consistent approach *Acta Mater.* **45** 4823–34
*Castelnau O, Duval P, Lebensohn R A and Canova G R 1996a Viscoplastic modelling of texture development in polycrystalline ice with a self-consistent approach; comparison with bound estimates *J. Geophys. Res.* **101** 13 851–68
*Castelnau O, Thorsteinsson T, Kipfstuhl J, Duval P and Canova G R 1996b Modelling fabric development along the GRIP ice core (central Greenland) *Anal. Glaciol.* **23** 194–201
*Chastel Y B, Dawson P R, Wenk H-R and Bennett K 1993 Anisotropic convection with implications for the upper mantle *J. Geophys. Res.* B **98** 17 757–71
Crampin S 1981 A review of wave motion in anisotropic and cracked elastic media *Wave Motion* **3** 242–391
Dawson P R and Beaudoin A J 1998 Finite element modelling of heterogeneous plasticity *Texture and Anisotropy. Preferred Orientation in Polycrystals and their Effect on Material Properties* ed U Kocks *et al* (Cambridge: Cambridge University Press) pp 513–31
Dawson P R and Wenk H-R 1999 Texturing of the upper mantle during convection *Phil. Mag.* in press
De Bresser J H P and Spiers C J 1997 Strength characteristics of the r, f and c slip systems in calcite *Tectonophys.* **272** 1–23.
Dell'Angelo L N and Tullis J 1989 Fabric development in experimentally sheared quartzites *Tectonophys.* **169** 1–21
Dietrich D and Song H 1984 Calcite fabrics in a natural shear environment; the Helvetic nappes of western Switzerland *J. Struct. Geol.* **6** 19–32
Duval P 1981 Creep and fabrics of polycrystalline ice under shear and compression *J. Glaciol.* **27** 129–40
Duval P and Castelnau O 1995 Dynamic recrystallization of ice in polar ice sheets *J. Phys. C: Solid State Phys.* **5** 197–205
*Erskine B G, Heidelbach F and Wenk H-R 1993 Lattice preferred orientations and microstructures of deformed Cordilleran marbles: correlation of shear indicators and determination of strain path *J. Struct. Geol.* **15** 1189–205
Frost H J and Ashby M F 1982 *Deformation Mechanism Maps. The Plasticity and Creep of Metals and Ceramics* (Oxford: Pergamon)
Hager B H and O'Connell R J 1981 A simple global model of plate dynamics and mantle convection *J. Geophys. Res.* **86** 4843–67
Herron S L and Langway C C 1982 A comparison of ice textures and fabrics at Camp Century, Greenland and Byrd Station, Antarctica *Ann. Glaciol.* **3** 118–24
Hess H H 1964 Seismic anisotropy of the uppermost mantle under oceans *Nature* **203** 629
Hosford W F 1964 Microstructural changes during deformation of [110]-fiber textured metals *Trans. Metall. Soc. AIME* **230** 12–15
Kamb W B 1959 Ice petrofabric observations from Blue Glacier, Washington, in relation to theory and experiment *J. Geophys. Res.* **64** 1891–909
Kern H 1971 Dreiaxiale Verformungen an Solnhofen Kalkstein im Temperaturbereich von 20 °C–650 °C. Röntgenographische Gefügeuntersuchungen mit dem Texturgoniometer *Contrib. Mineral. Petrol.* **31** 39–66
Kern H and Wenk H-R 1990 Fabric-related velocity anisotropy and shear wave splitting in rocks from the Santa Rosa mylonite zone, California *J. Geophys. Res.* **95** 11 213–23
Kocks U F, Tomé C N and Wenk H-R 1998 *Texture and Anisotropy. Preferred Orientation in Polycrystals and their Effect on Material Properties* (Cambridge: Cambridge University Press)

*Kunze K, Pieri M, Burlini L and Wenk H-R 1998 Texture development in calcite during deformation and recrystallization. Interpretation of high strain torsion experiments *Trans. Am. Geophys.* 79

Law R D 1990 Crystallographic fabrics: a selective review of their applications to research in structural geology *Deformation Mechanisms, Rheology and Tectonics* vol 54, ed R J Knipe and E H Rutter (London: Geological Society) pp 335–52

*Lebensohn R A, Gonzalez M I, Tomé C N and Pochettino A A 1996 Measurement and prediction of texture development during a rolling sequence of zircaloy-4 tubes *J. Nucl. Mater.* **229** 57–64

*Lebensohn R A, Sanchez P V and Pochettino A A 1994 Modelling texture development of zirconium alloys at high temperatures *Scripta Metall. Mater.* **30** 481–6

*Lebensohn R A and Tomé C N 1993 A self-consistent anisotropic approach for the simulation of plastic deformation and texture development of polycrystals—application to zirconium alloys *Acta Metall. Mater.* **41** 2611–24

——1994 A self-consistent visco-plastic model: prediction of rolling textures of anisotropic polycrystals *Mater. Sci. Eng.* A **175** 71–82

*Lebensohn RA, Wenk H-R and Tomé CN 1998 Modelling deformation and recrystallization textures in calcite *Acta Mater.* **46** 2683–93

Lipenkov V Y, Barkov N I, Duval P and Pimienta P 1989 Crystalline texture of the 2083m ice core at Vostok Station, Antarctica *J. Glaciol.* **35** 392–8

Lister G S and Hobbs B E 1980 The simulation of fabric development during plastic deformation and its application to quartzite: the influence of deformation history *J. Struct. Geol.* **2** 355–70

Lister G S, Paterson M S and Hobbs B E 1978 The simulation of fabric development during plastic deformation and its application to quartzite: the model *Tectonophys.* **45** 107–58

*Molinari A, Canova GR and Ahzi S 1987 A self-consistent approach of the large deformation polycrystal viscoplasticity *Acta Metall.* **35** 2983–94

*Molinari A and Tóth L S 1994 Tuning a self-consistent viscoplastic model by finite element results. Part I: Modeling *Acta Metall. Mater.* **42** 2453–8

Morris G B, Raitt R W and Shor G G 1969 Velocity anisotropy and delay time maps of the mantle near Hawaii *J. Geophys. Res.* **74** 4300–16

Nicolas A, Boudier F and Boullier A-M 1973 Mechanisms of flow in naturally and experimentally deformed peridotites *Am. J. Sci.* **273** 853–76

Nishimura C and Forsyth D 1989 The anisotropic structure of the upper mantle in the Pacific *Geophys. J.* **96** 203–29

Parks D M and Ahzi S 1990 Polycrystalline plastic deformation and texture evolution for crystals lacking five independent slip systems *J. Mech. Phys. Solids* **38** 701–24

Paterson M S and Weiss L E 1961 Symmetry concepts in the structural analysis of deformed rocks *Geol. Soc. Am. Bull.* **72** 841–2

*Ratschbacher L, Wenk H-R and Sintubin M 1991 Calcite textures: examples from nappes with strain-path partitioning. *J. Struct. Geol.* **13** 369–84

Sachs G 1928 Zur Ableitung einer Fliessbedingung *Z. Ver. Dtsch. Ing.* **72** 734–6

Schmidt W 1925 Gefügestatistik *Tschermaks Mineral. Petrog. Mitt.* **38** 392–423

Siemes H 1974 Anwendung der Taylor-Theorie auf die Regelung von kubischen Mineralen *Contrib. Mineral. Petrol.* **43** 149–57

Silver P G 1996 Seismic anisotropy beneath the continents: probing the depths of geology *Ann. Rev. Earth Planet. Sci.* **24** 385–432

Skrotzki W and Welch P 1983 Development of texture and microstructure in extruded ionic polycrystalline aggregates *Tectonophys.* **99** 47–62

Takeshita T, Tomé C N, Wenk H-R and Kocks U F 1987 Single crystal yield surface for trigonal lattices: application to texture transitions in calcite polycrystals *J. Geophys. Res.* B **92** 12 917–20

Takeshita T, Wenk H-R and Lebensohn R 1999 Development of preferred orientation and microstructure in sheared quartzite: comparison of natural and simulated data *Tectonophys.* in press

*Takeshita T, Wenk H-R, Molinari A and Canova G 1990 Simulation of dislocation assisted plastic deformation in olivine polycrystals *Deformation Processes in Minerals, Ceramics and Rocks* ed D J Barber and P G Meredith (London: Unwin Hyman) pp 365–77

Taylor G I 1938a Plastic strain in metals *J. Inst. Met.* **62** 307–24

Tison J-L, Thorsteinsson T, Lorrain R D and Kipfstuhl J 1994 Origin and development of textures and fabrics in basal ice at Summit, Central Greenland *Earth Planet. Sci. Lett.* **125** 421–37

Tomé C N and Canova G R 1998 Self-consistent modeling of heterogeneous plasticity *Texture and Anisotropy: Preferred Orientations in Polycrystals and Their Effect on Materials Properties* ed U Kocks *et al* (Cambridge: Cambridge University Press) pp 466–510

*Tomé C N, Wenk H-R, Canova G R and Kocks U F 1991b Simulations of texture development in calcite: comparison

of polycrystal plasticity theories *J. Geophys. Res.* **96** 11 865–75
*Tommasi A, Vauchez A, Mainprice D, Russo R and Canova G 1997 Forward modelling of the development of seismic anisotropy in ocean basins through resistive drag of sublithospheric mantle *Trans. Am. Geophys.* **78**
Tullis J and Wenk H-R 1994 The effect of muscovite on the strength and lattice preferred orientations of experimentally deformed quartz aggregates *Mater. Sci. Eng.* A **175** 209–20
Vinnik L, Romanowicz B and Breger L 1994 Anisotropy in the center of the inner core *Geophys. Res. Lett.* **21** 1671–4
Wenk H R 1985 Carbonates preferred orientation in deformed metals and rocks *An Introduction to Modern Texture Analysis* ed H-R Wenk (Orlando, FL: Academic) pp 361–84
——1994 Preferred orientation patterns in deformed quartzites *Reviews in Mineralogy vol 29, Silica Physical Behavior, Geochemistry and Materials Applications* ec P J C T Prewitt and G V Gibbs (Washington, DC: Mineral Society of America) pp 177–208
*——1998 Plasticity modeling in minerals and rocks *Texture and Anisotropy: Preferred Orientations in Polycrystals and Their Effect on Materials Properties* ed U Kocks *et al* (Cambridge: Cambridge University Press) pp 560–95
*Wenk H-R, Baumgardner J, Lebensohn R A and Tomé C N 1999a Can convection of the inner core produce anisotropy? *J. Geophys. Res.* submitted
*Wenk H-R, Bennett K, Canova G and Molinari A 1991 Modelling plastic deformation of peridotite with the self-consistent theory *J. Geophys. Res.* B **96** 8337–49
*Wenk H-R, Canova G C, Brechet Y and Flandin L 1997 A deformation-based model for recrystallization of anisotropic materials *Acta Mater.* **45** 3283–96
*Wenk H-R, Canova G, Molinari A and Kocks U F 1989a Viscoplastic modelling of texture development in quartzite *J. Geophys. Res.* **94** 17 895–906
*Wenk H-R, Canova G, Molinari A and Mecking H 1989b Texture development in halite: comparison of Taylor model and self-consistent theory *Acta Metall.* **37** 2017–29
Wenk H-R, Dawson P, Pelkie C and Chastel Y 1999b *Texturing of Rocks in the Earth's Mantle. A Convection Model Based on Polycrystal Plasticity* (Video, AGU) submitted
Wenk H-R, Kern H, Van Houtte P and Wagner F 1986 Heterogeneous strain in axial deformation of limestone, textural evidence *Mineral and Rock Deformation: Laboratory Studies* ed B E Hobbs and H C Heard *Am. Geoph. U. Geophys. Monogr.* **36** 287–95
Wenk H-R, Takeshita T, Bechler E, Erskine B G and Matthies S 1987 Pure shear and simple shear calcite textures. Comparison of experimental, theoretical and natural data *J. Struct. Geol.* **9** 731–45
*Wenk H-R and Tomé C N 1999 Modeling recrystallization of olivine in simple shear *J. Geophys. Res.* in press
Wenk H-R, Venkitasubramanyan C S, Baker D W and Turner F J 1973 Preferred orientation in experimentally deformed limestone *Contrib. Mineral. Petrol.* **38** 81–114
Woodhouse J H, Giardini D and Li X-D 1986 Evidence for inner core anisotropy from free oscillations *Geophys. Res. Lett.* **13** 1549–52
Zhang S and Karato S-Y 1995 Lattice preferred orientation of olivine aggregates deformed in simple shear *Nature* **375** 774–7